is one of the common pathomechanisms of various neurodegenerative diseases, including Alzheimer's disease (AD), Parkinson's disease (PD) and polyglutamine diseases.[10] Recently, several investigators have reported that familial ALS-associated proteins (trans-activation response DNA protein 43 (TDP-43),[11–14] fused in sarcoma (FUS),[15,16] optineurin,[17,18] ubiquilin-2,[19,20] charged mutivesicular body protein 2b (CHMP2B)[21,22] and valosin-containing protein[23]) are involved in inclusion body formation in various neurodegenerative diseases. These reports prompted us to investigate whether FIG4 is involved in a variety of neurodegenerative diseases, including TDP-43 proteinopathy (sporadic ALS and frontotemporal lobar degeneration). Using immunohistochemistry, we therefore examined the brains and spinal cords of patients with various neurodegenerative diseases and control subjects using anti-FIG4 antibody. Here we report that FIG4 is not incorporated in TDP-43 inclusions and that FIG4 immunoreactivity is present in Pick bodies in Pick's disease, Lewy bodies in PD and dementia with Lewy bodies (DLB), and neuronal nuclear inclusions (NNIs) in polyglutamine and intranuclear inclusion body diseases.

MATERIALS AND METHODS

Subjects

Seventy-four autopsy cases were investigated in this study; these included cases of sporadic ALS ($n = 5$), frontotemporal lobar degeneration with TDP-43-positive inclusions (FTLD-TDP type B; $n = 5$),[24] AD ($n = 5$), Pick's disease ($n = 4$), progressive supranuclear palsy (PSP; $n = 4$), corticobasal degeneration (CBD; $n = 4$), argyrophilic grain disease (AGD; $n = 4$), PD ($n = 5$), neocortical-type DLB ($n = 5$), multiple system atrophy (MSA; $n = 5$), dentatorubral-pallidoluysian atrophy (DRPLA; $n = 3$), Huntington's disease (HD; $n = 5$), spinocerebellar ataxia type 1 (SCA1; $n = 3$), SCA2 ($n = 1$),[13] SCA3 ($n = 5$), intranuclear inclusion body disease (INIBD; $n = 5$) and normal controls (aged 48–84 years, average 63.8 years, $n = 6$). All the diagnoses had been confirmed by neuropathological examinations using immunohistochemistry for tau, β-amyloid, α-synuclein, TDP-43, polyglutamine and ubiquitin. This study was approved by the Institutional Ethics Committee of Hirosaki University Graduate School of Medicine.

Immunohistochemistry

Immunohistochemical analysis was carried out using formalin-fixed, paraffin-embedded sections from the frontal cortex, hippocampus, basal ganglia, midbrain, pons, medulla oblongata, cerebellum, spinal cord, and sympathetic and spinal ganglia of normal controls. In other cases, multiple sections taken from the affected regions were immunostained; the frontal cortex and hippocampus in FTLD-TDP, AD, Pick's disease, CBD, DLB, SCA1 and INIBD, the amygdaloid nucleus and hippocampus in AGD, the basal ganglia in HD and SCA2, the midbrain in PSP, PD and DLB, the pons in MSA, DRPLA and SCA3, and the motor cortex and spinal cord in ALS. The sections were initially subjected to heat retrieval for 10 min in 10 mmol/L citrate buffer (pH 6.0) using an autoclave, and then subjected to immunohistochemical processing using the avidin-biotin-peroxidase complex method with diaminobenzidine. The primary antibody used was a rabbit polyclonal anti-FIG4 antibody (CAB017823 in The Human Protein Atlas; Novus Biologicals, Littleton, CO, USA; 1:300).

Double immunofluorescence analysis was performed to detect overlapping expression of FIG4 and phosphorylated tau, phosphorylated α-synuclein, polyglutamine or ubiquitin. Paraffin sections from the hippocampus of patients with Pick's disease and DLB, the midbrain of patients with PD, the pons of patients with DRPLA and SCA3, and the frontal cortex of patients with INIBD were processed for double-label immunofluorescence. De-paraffinized sections were blocked with donkey serum and then incubated overnight at 4°C with a mixture of polyclonal anti-FIG4 (1:100) and monoclonal anti-phosphorylated tau (AT8; Innogenetics, Ghent, Belgium; 1:200) for Pick's disease, anti-phosphorylated α-synuclein (#64; Wako, Osaka, Japan; 1:1000) for PD and DLB, anti-polyglutamine (1C2; Chemicon, Temecula, CA, USA; 1:40) for DRPLA and SCA3, or anti-ubiquitin (1B3; MBL, Nagoya, Japan; 1:400) for INIBD. The sections were then rinsed and incubated with anti-rabbit IgG tagged with Alexa Fluora 488 (Invitrogen, Carlsbad, CA, USA; 1:1000) or anti-mouse IgG tagged with Alexa Fluora 594 (Invitrogen; 1:1000) for 1 h at 38°C. The sections were mounted using ProLong gold antifade reagent with 4′,6-diamino-2-phenylindole (DAPI; Invitrogen) and examined with a confocal microscope (EZ-Ci; Nikon, Tokyo, Japan). The proportion of FIG4-positive inclusions relative to the total number of inclusions positive for phosphorylated tau, phosphorylated α-synuclein, polyglutamine or ubiquitin was calculated in each case. Values were expressed as the mean for each diagnostic group.

RESULTS

FIG4 immunoreactivity in normal controls

In normal controls, anti-FIG4 antibody immunolabeled the neuronal cytoplasm in a diffuse granular pattern throughout the CNS, including the cerebral cortex (Fig. 1A), hippocampus (Fig. 1B), basal ganglia (Fig. 1C),

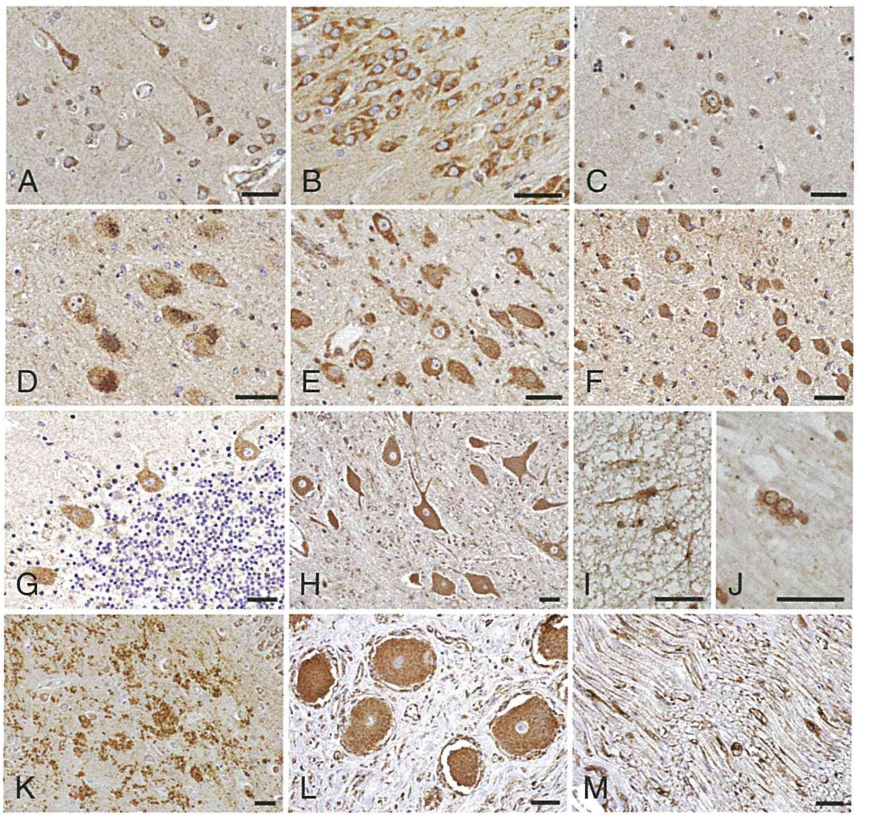

Fig. 1 FIG4 immunoreactivity in the normal human nervous system. The neuronal cytoplasm in the frontal cortex (A), dentate gyrus (B), putamen (C), substantia nigra (D), pontine nucleus (E), inferior olivary nucleus (F), cerebellar cortex (G) and anterior horn of the lumbar cord (H) showing FIG4 immunoreactivity. The cytoplasm of astrocytes in the periaqueductal white matter (I) and oligodendrocytes in the pontine base (J) showing weak FIG4 immunoreactivity. Strong FIG4 immunoreactivity is evident in mossy fiber terminals in the hippocampal CA4 region (K). Ganglion cells and satellite cells in the spinal ganglia (L) and Schwann cells in the peripheral nerves (M) showing FIG4 immunoreactivity. Bars = 40 μm.

brainstem (Fig. 1D–F), cerebellum (Fig. 1G) and spinal cord (Fig. 1H). The cytoplasm of astrocytes and oligodendrocytes was also weakly immunostained with anti-FIG4 (Fig. 1I,J). Although axons and presynaptic nerve terminals were barely immunolabeled or unstained, mossy fiber terminals (axon terminals of dentate granule cells) were intensely immunolabeled (Fig. 1K). In the sympathetic and spinal ganglia, the cytoplasm of ganglion cells, satellite cells and Schwann cells was immunostained (Fig. 1L,M). Neuronal and glial nuclei were not stained with anti-FIG4 antibody.

FIG4 immunoreactivity in neurodegenerative diseases

Although TDP-43-positive neuronal and glial cytoplasmic inclusions were found in the cerebral cortex in FTLD-TDP and the upper and lower motor neuron systems in ALS, no FIG4-immunoreactive inclusions were noted in these areas (data not shown).

In AD, dystrophic neurites in senile plaques were positive for FIG4 (Fig. 2A). In Pick's disease, Pick bodies were intensely immunostained with anti-FIG4 (Fig. 2B). However, no FIG4 immunoreactivity was found in NFTs in AD, PSP and CBD, argyrophilic grains in AGD, tufted astrocytes in PSP, or astrocytic plaques in CBD.

In PD and DLB, the majority of brainstem-type Lewy bodies were positive for FIG4 (Fig. 2C). A small fraction of cortical Lewy bodies were also positive for FIG4 (Fig. 2D). Both brainstem-type and cortical Lewy bodies showed intense staining in their central portion, whereas the peripheral portion was not stained with anti-FIG4. Pale bodies, which have been considered precursors of Lewy bodies,[25] and intraneuritic Lewy bodies (Lewy neurites) were negative for FIG4. In MSA, glial cytoplasmic inclusions, glial nuclear inclusions, neuronal cytoplasmic inclusions, neuronal nuclear inclusions and swollen neurites were intensely immunolabeled with anti-phosphorylated α-synuclein.[26] However, these structures were FIG4-negative.

Immunohistochemistry for ubiquitin and polyglutamine revealed NNIs in all of the cases of polyglutamine diseases examined. NNIs in DRPLA and SCA3, but not in HD, SCA1 and SCA2, were immunolabeled with anti-FIG4 (Fig. 2E,F).

In INIBD, ubiquitin-positive nuclear inclusions were found in both neurons and glial cells. FIG4 immunoreactivity was present in nuclear inclusions in neurons (Fig. 2G), but not in glial cells.

In aged normal controls and patients with neurodegenerative diseases, Marinesco bodies were observed in the nuclei of substantia nigra pigmented neurons, and were

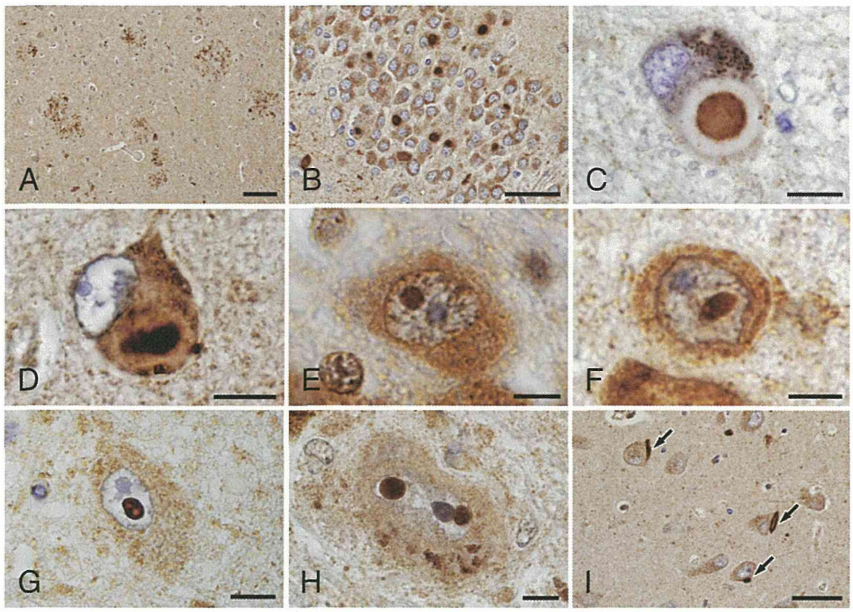

Fig. 2 FIG4 immunoreactivity in neurodegenerative diseases. Neuritic plaques in the hippocampus of Alzheimer's disease (A). Pick bodies in the dentate granule cells of Pick's disease (B). Lewy bodies in the substantia nigra of Parkinson's disease (C) and temporal cortex of dementia with Lewy bodies (D). (E–G) Neuronal nuclear inclusions in the pons of dentatorubral-pallidoluysian atrophy (DRPLA) (E) and spinocerebellar ataxia type 3 (SCA3) (F), and in the frontal cortex of intranuclear inclusion body disease (INIBD) (G). Marinesco bodies in the substantia nigra (H) and Hirano bodies (arrows) in the hippocampus (I) of control subjects. Bars = 100 μm (A), 40 μm (B, I), 10 μm (C–H).

strongly positive for FIG4 (Fig. 2H). In addition, Hirano bodies in the hippocampus were FIG4 positive (Fig. 2I).

There was no apparent difference in the staining intensity of neuronal cytoplasms with and without inclusions between patients with neurodegenerative diseases and normal controls.

Double immunofluorescence analysis

Double immunofluorescence analysis revealed co-localization of FIG4 and phosphorylated tau in Pick bodies (Fig. 3A–C) and neuropil threads (Fig. 3D–F) in Pick's disease, the latter corresponding to small Pick bodies in the neurites.[27,28] The average proportion of FIG4-positive Pick bodies relative to the total number of inclusions was 88.7%. In both brainstem-type and cortical Lewy bodies, FIG4 immunoreactivity was concentrated in the central portion and α-synuclein immunoreactivity was more intense in the peripheral portion (Fig. 3G–L). The average proportion of FIG4-positive brainstem-type and cortical Lewy bodies relative to the total number of inclusions was 88.9% and 45.3%, respectively. Co-localization of FIG4 with polyglutamine or ubiquitin was demonstrated in NNIs in DRPLA (Fig. 3M–O), SCA3 (Fig. 3P–R) and INIBD (Fig. 3S–U). The FIG4 positivity rate of NNIs in DRPLA, SCA3 and INIBD was 19.5%, 19.7% and 28.6%, respectively. Almost all Marinesco bodies (99.8%) were positive for FIG4.

DISCUSSION

In rodents, FIG4 is abundantly expressed in neurons and myelin-forming cells in the central and peripheral nervous systems during neural development, and is markedly diminished in neurons of the adult CNS.[4] In the present study, we demonstrated that FIG4 immunoreactivity was present in neuronal cytoplasm in the brain, spinal cord and peripheral ganglia of adult humans. Schwann cells in the peripheral nervous system were also strongly immunolabeled with anti-FIG4, whereas oligodendrocytes and astrocytes in the CNS were weakly positive. These findings suggest that FIG4 is widely expressed in neurons and glial cells throughout the adult human nervous system.

In the present study, no FIG4 immunoreactivity was found in a variety of neuronal and glial inclusions in sporadic TDP-43 proteinopathy (ALS and FTLD-TDP type B). Although TDP-43-positive neuronal and glial cytoplasmic inclusions have been found in a previous case of SCA2,[13] no FIG4-immunoreactive inclusions were noted in that case. Our data indicate that FIG4 is not incorporated into TDP-43 inclusions.

We further demonstrated that the majority of Pick bodies were immunopositive for FIG4. Considering that dentate granule cells are one of the sites where Pick bodies accumulate preferentially, it is important to note that the cytoplasm and axon terminals of dentate granule cells were strongly positive for FIG4. Previous immunohistochemical studies have shown that Pick bodies are immunoreactive for synaptic proteins.[29] These findings suggest that the proteins synthesized in neuronal perikarya might be entrapped within the filamentous structure of Pick bodies. However, in the present study Pick bodies present inside and outside the dentate gyrus were intensely immunolabeled with anti-FIG4. Moreover, co-localization of FIG4 and phosphorylated tau was seen in the neuropil, which

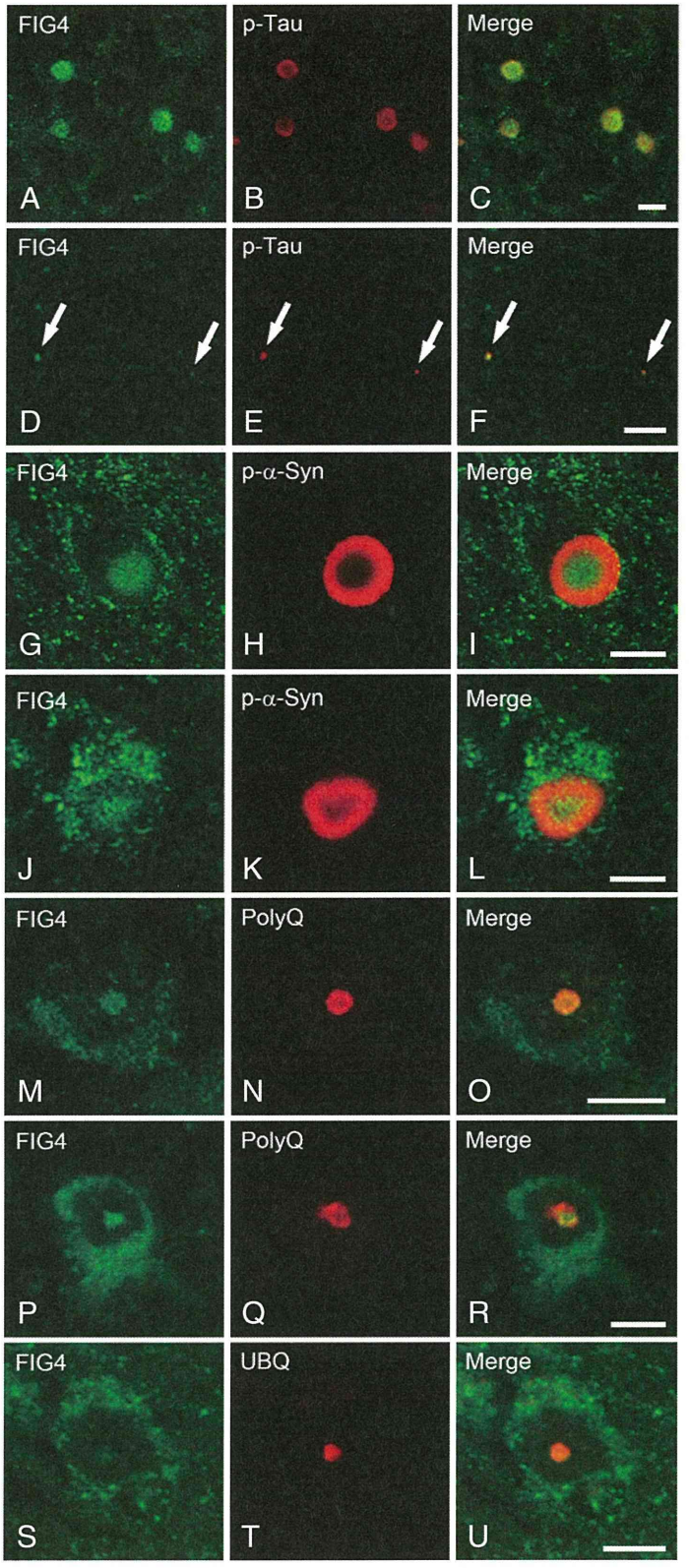

Fig. 3 Double-labeling immunofluorescence demonstrating co-localization of FIG4 and phosphorylated tau (p-Tau) in Pick bodies (A–C) and neuropil threads (D–F) (arrows) in the dentate gyrus of Pick's disease, FIG4 and phosphorylated α-synuclein (p-α-Syn) in nigral (G–I) and cortical (J–L) Lewy bodies, FIG4 and polyglutamine (PolyQ) or ubiquitin (UBQ) in neuronal nuclear inclusions of dentatorubral-pallidoluysian atrophy (DRPLA) (M–O), spinocerebellar ataxia type 3 (SCA3) (P–R) and intranuclear inclusion body disease (INIBD) (S–U). FIG4 appears *green* (A,D,G,J,M,P,S) and p-Tau (B,E), p-α-Syn (H,K), PolyQ (N,Q) or UBQ (T) appears *red*. Overlap of FIG4 with p-Tau, p-α-Syn, PolyQ or UBQ appears *yellow* (merge). Bars = 10 μm.

corresponds to small Pick bodies in the neurites.[27,28] It seems likely that incorporation of FIG4 into Pick bodies is a pathological event, and does not simply reflect entrapment of the protein.

Lewy bodies consist of a dense core and a peripheral halo, which correspond ultrastructurally to zones of densely compacted circular profiles and zones of filaments, respectively.[30] It is well known that the constituent filaments of Lewy bodies are composed of α-synuclein. However, little is known about the components of the central core of Lewy bodies. In the present study, the cores of brainstem-type and cortical Lewy bodies were immunolabeled intensely by anti-FIG4 antibody, but their peripheral portions were only weakly stained or unstained. This localization implies that FIG4 is involved in formation of the central core of Lewy bodies and that FIG4 may not interact with α-synuclein.

In polyglutamine diseases, NNIs in DRPLA and SCA3, but not in HD, SCA1 and SCA2, were immunopositive for FIG4. NNIs in INIBD were also positive for FIG4. In addition to the cytoplasm, FIG4 is reportedly localized in the nuclear pore, being required for efficient export of nuclear signal-containing reporter protein.[31] This interaction is thought to be important for the regulation of gene expression or DNA synthesis.[30] In polyglutamine diseases, NNIs may affect nuclear function and recruitment of other proteins, possibly resulting in loss of the physiological function of recruited proteins, and subsequent neuronal dysfunction.[32] Similar mechanisms may occur in the pathogenesis of INIBD, although the major component of nuclear inclusions in this disease is uncertain. It is possible that FIG4 translocates from the cytoplasm to the nucleus in order to protect cells from cytotoxic events. However, it is unclear why only two polyglutamine diseases (DRPLA and SCA3) showed FIG4 immunoreactivity in NNIs. The evidence suggests that the mechanism of inclusion body formation may differ among the various polyglutamine diseases.

In the present study, Marinesco bodies were also immunoreactive for FIG4. The frequency of Marinesco bodies is significantly higher in nigral neurons with Lewy bodies than in those without.[33] The melanin content of nigral neurons containing Marinesco bodies is lower than that of nigral neurons lacking Marinesco bodies.[34] The available evidence suggests that Marinesco bodies may play a pathogenic role in certain neurodegenerative disorders, and that the formation and disaggregation of Marinesco bodies are features common to the disease process of neurodegenerative conditions characterized by the presence of intranuclear inclusions.[35]

Mutations of *FIG4* result in the accumulation of enlarged vesicles derived from the endosomal-lysosomal pathway in the central and peripheral nervous systems of FIG4-mutated mice.[6] A similar phenomenon is evident in fibroblasts from patients with CMT4J, suggesting impaired trafficking of intracellular organelles due to physical obstruction by vacuoles.[7] FIG4 has not been directly implicated in autophagy, whereas a role for phosphatidylinositol-3-phosphate, which is both a metabolic precursor and a product of phosphatidylinositol 3,5-bisphosphate, is involved in autophagy.[36] This implies the involvement of FIG4 in both the endosomal-lysosomal and autophagy-lysosomal pathways.[37] Lázaro-Diéguez *et al.* have reported that in a variety of mammalian cells the reversible formation of filamentous actin-enriched aggresomes is generated by the actin toxin jasplakinolide.[38] Notably, these aggresomes resemble Hirano bodies observed in the human brain in many respects. Moreover, Hirano bodies are immunopositive for ubiquilin-1.[39] The available evidence suggests that ubiquilin-1 exerts a cytoprotective role by targeting polyubiquitinated proteins for proteasomal degradation or the action of autophagosomes, or by sequestering aggregated proteins to aggresomes.[40–44] The above findings suggest that Hirano bodies may represent autophagy- and/or aggresome-related structures.

In conclusion, we have demonstrated for the first time that FIG4 immunoreactivity is present in Pick bodies in Pick's disease, Lewy bodies in PD and DLB, and NNIs in polyglutamine and intranuclear inclusion body diseases. These findings suggest that FIG4 may have a common role in the formation or degradation of neuronal cytoplasmic and nuclear inclusions in several neurodegenerative diseases.

ACKNOWLEDGMENTS

This work was supported by JSPS KAKENHI Grant Number 23500424 (F.M.), 23500425 (K.T.) and 24300131 (K.W.), Grants for Priority Research Designated by the President of Hirosaki University (K.T., K.W.), the Collaborative Research Project (2013-2508) of the Brain Research Institute, Niigata University (F.M.), Grants-in Aid from the Research Committee for Ataxic Disease, the Ministry of Health, Labour and Welfare, Japan (H.S., K.W.), and the Intramural Research Grant (24-5) for Neurological and Psychiatric Disorders of NCNP (K.W.). The authors wish to express their gratitude to M. Nakata for her technical assistance.

REFERENCES

1. Nagase T, Seki N, Ishikawa K *et al.* Prediction of the coding sequences of unidentified human genes. VI. The coding sequences of 80 new genes (KIAA0201-KIAA0280) deduced by analysis of cDNA clones from cell line KG-1 and brain. *DNA Res* 1996; **3**: 321–329.

2. Erdman S, Lin L, Malczynski M, Snyder M. Pheromone-regulated genes required for yeast mating differentiation. *J Cell Biol* 1998; **140**: 461–483.
3. Winters JJ, Ferguson CJ, Lenk GM *et al.* Congenital CNS hypomyelination in the *Fig4* null mouse is rescued by neuronal expression of the PI(3,5)P phosphatase *Fig4*. *J Neurosci* 2011; **31**: 17736–17751.
4. Guo J, Ma YH, Yan Q *et al.* Fig4 expression in the rodent nervous system and its potential role in preventing abnormal lysosomal accumulation. *J Neuropathol Exp Neurol* 2012; **71**: 28–39.
5. Ferguson CJ, Lenk GM, Jones JM *et al.* Neuronal expression of *Fig4* is both necessary and sufficient to prevent spongiform neurodegeneration. *Hum Mol Genet* 2012; **21**: 3525–3534.
6. Chow CY, Zhang Y, Dowling JJ *et al.* Mutation of *FIG4* causes neurodegeneration in the pale tremor mouse and patients with CMT4J. *Nature* 2007; **448**: 68–72.
7. Zhang X, Chow CY, Sahenk Z, Shy ME, Meisler MH, Li J. Mutation of *FIG4* causes a rapidly progressive, asymmetric neuronal degeneration. *Brain* 2008; **131**: 1990–2001.
8. Chow CY, Landers JE, Bergren SK *et al.* Deleterious variants of *FIG4*, a phosphoinositide phosphatase, in patients with ALS. *Am J Hum Genet* 2009; **84**: 85–88.
9. Takalo M, Salminen A, Soininen H, Hiltunen M, Haapasalo A. Protein aggregation and degradation mechanisms in neurodegenerative diseases. *Am J Neurodegener Dis* 2013; **2**: 1–14.
10. Martinez-Vicente M, Cuervo AM. Autophagy and neurodegeneration: when the cleaning crew goes on strike. *Lancet Neurol* 2007; **6**: 352–361.
11. Arai T, Mackenzie IR, Hasegawa M *et al.* Phosphorylated TDP-43 in Alzheimer's disease and dementia with Lewy bodies. *Acta Neuropathol* 2009; **117**: 125–136.
12. Tan C-F, Yamada M, Toyoshima Y *et al.* Selective occurrence of TDP-43-immunoreactive inclusions in the lower motor neurons in Machado-Joseph disease. *Acta Neuropathol* 2009; **118**: 553–560.
13. Toyoshima Y, Tanaka H, Shimohata M *et al.* Spinocerebellar ataxia type 2 (SCA2) is associated with TDP-43 pathology. *Acta Neuropathol* 2011; **122**: 375–378.
14. Blokhuis AM, Groen EJN, Koppers M, van den Berg LH, Pasterkamp RJ. Protein aggregation in amyotrophic lateral sclerosis. *Acta Neuropathol* 2013; **125**: 777–794.
15. Woulfe J, Gray DA, Mackenzie IR. FUS-immunoreactive intranuclear inclusions in neurodegenerative disease. *Brain Pathol* 2010; **20**: 589–597.
16. Mori F, Tanji K, Kon T *et al.* FUS immunoreactivity of neuronal and glial intranuclear inclusions in intranuclear inclusion body disease. *Neuropathol Appl Neurobiol* 2012; **38**: 322–328.
17. Osawa T, Mizuno Y, Fujita Y, Takatama M, Nakazato Y, Okamoto K. Optineurin in neurodegenerative diseases. *Neuropathology* 2011; **31**: 569–574.
18. Mori F, Tanji K, Toyoshima Y *et al.* Optineurin immunoreactivity in neuronal nuclear inclusions of polyglutamine diseases (Huntington's, DRPLA, SCA2, SCA3) and intranuclear inclusion body disease. *Acta Neuropathol* 2012; **123**: 747–749.
19. Brettschneider J, Van Deerlin VM, Robinson JL *et al.* Pattern of ubiquilin pathology in ALS and FTLD indicates presence of C9ORF72 hexanucleotide expansion. *Acta Neuropathol* 2012; **123**: 825–839.
20. Mori F, Tanji K, Odagiri S *et al.* Ubiquilin immunoreactivity in cytoplasmic and nuclear inclusions in synucleinopathies, polyglutamine diseases and intranuclear inclusion body disease. *Acta Neuropathol* 2012; **124**: 149–151.
21. Tanikawa S, Mori F, Tanji K, Kakita A, Takahashi H, Wakabayashi K. Endosomal sorting related protein CHMP2B is localized in Lewy bodies and glial cytoplasmic inclusions in α-synucleinopathy. *Neurosci Lett* 2012; **527**: 16–21.
22. Kurashige T, Takahashi T, Yamazaki Y *et al.* Localization of CHMP2B-immunoreactivity in the brainstem of Lewy body disease. *Neuropathology* 2013; **33**: 237–245.
23. Mori F, Tanji K, Toyoshima Y *et al.* Valosin-containing protein immunoreactivity in tauopathies, synucleinopathies, polyglutamine diseases and intranuclear inclusion body disease. *Neuropathology* 2013; **33**: 637–644.
24. Mackenzie IR, Neumann M, Baborie A *et al.* A harmonized classification system for FTLD-TDP pathology. *Acta Neuropathol* 2011; **122**: 111–113.
25. Wakabayashi K, Hayashi S, Kakita A *et al.* Accumulation of α-synuclein/NACP is a cytopathological feature common to Lewy body disease and multiple system atrophy. *Acta Neuropathol* 1998; **96**: 445–452.
26. Nishie M, Mori F, Fujiwara H *et al.* Accumulation of phosphorylated α-synuclein in the brain and peripheral ganglia of patients with multiple system atrophy. *Acta Neuropathol* 2004; **107**: 292–298.
27. Oyanagi S, Tanaka M, Omori T, Matsushita M, Ishii T. Regular arrangements of tubular structures in Pick bodies formed in an autopsied case of Pick's disease (in Japanese with English abstract). *Shinkei Simpo* 1979; **23**: 441–451.
28. Oyanagi S. *A Guide to Neuropathology by Electron Microscopy*, 1st edn. Tokyo: Igaku Shoin, 1992.
29. Mori F, Hayashi S, Yamagishi S *et al.* Pick's disease: α- and β-synuclein-immunoreactive Pick bodies in the

dentate gyrus. *Acta Neuropathol* 2002; **104**: 455–461.
30. Duffy PE, Tennyson VM. Phase and electron microscopic observations of Lewy bodies and melanin granules in the substantia nigra and locus caeruleus in Parkinson's disease. *J Neuropathol Exp Neurol* 1965; **24**: 398–414.
31. Jones AL, Quimby BB, Hood JK *et al. SAC3* may link nuclear protein export to cell cycle progression. *Proc Natl Acad Sci USA* 2000; **97**: 3224–3229.
32. Takahashi T, Katada S, Onodera O. Polyglutamine diseases: where does toxicity come from? What is toxicity? Where are we going? *J Mol Cell Biol* 2010; **2**: 180–191.
33. Beach TG, Walker DG, Sue LL, Newell A, Adler CC, Joyce JN. Substantia nigra Marinesco bodies are associated with decreased striatal expression of dopaminergic markers. *J Neuropathol Exp Neurol* 2004; **63**: 329–337.
34. Ikeda K. A study of the Marinesco body in monkey (Macaca fuscata). A comparative study to the Marinesco body in man (in Japanese with English abstract). *Seishin Shinkeigaku Zasshi* 1974; **76**: 778–792.
35. Odagiri S, Tanji K, Mori F *et al.* Immunohistochemical analysis of Marinesco bodies, using antibodies against proteins implicated in the ubiquitin-proteasome system, autophagy and aggresome formation. *Neuropathology* 2012; **32**: 261–266.
36. Suzuki K, Ohsumi Y. Molecular machinery of autophagosome formation in yeast, Saccharomyces cerevisiae. *FEBS Lett* 2007; **581**: 2156–2161.
37. Volpicelli-Daley L, De Camilli P. Phosphoinositides link to neurodegeneration. *Nat Med* 2007; **13**: 784–786.
38. Lázaro-Diéguez F, Knecht E, Egea G. Clearance of a Hirano body-like F-actin aggresome generated by jasplakinolide. *Autophagy* 2008; **4**: 717–720.
39. Satoh J, Tabunoki H, Ishida T, Saito Y, Arima K. Ubiquilin-1 immunoreactivity is concentrated on Hirano bodies and dystrophic neuritis in Alzhermer's disease brains. *Neuropathol Appl Neurobiol* 2013. doi: 10.1111/nan.12036
40. Heir R, Ablasou C, Dumontier E, Elliott M, Fagotto-Kaufmann C, Bedford FK. The UBL domain of PLIC-1 regulates aggresome formation. *EMBO Rep* 2006; **7**: 1252–1258.
41. Viswanathan J, Haapasalo A, Böttcher C *et al.* Alzheimer's disease-associated ubiquilin-1 regulates presenilin-1 accumulation and aggresome formation. *Traffic* 2011; **12**: 330–348.
42. Rothenberg C, Srinivasan D, Mah L *et al.* Ubiquilin functions in autophagy and is degraded by chaperone-mediated autophagy. *Hum Mol Genet* 2010; **19**: 3219–3232.
43. Johansen T, Lamark T. Selective autophagy mediated by autophagic adapter proteins. *Autophagy* 2011; **7**: 279–296.
44. N'Diaye EN, Kajihara KK, Hsieh I, Morisaki H, Debnath J, Brown EJ. PLIC proteins or ubiquilins regulate autophagy-dependent cell survival during nutrient starvation. *EMBO Rep* 2009; **10**: 173–179.

Genes to Cells

Dab1-mediated colocalization of multi-adaptor protein CIN85 with Reelin receptors, ApoER2 and VLDLR, in neurons

Takahiro Fuchigami[1], Yutaka Sato[1a], Yuya Tomita[1], Tetsuya Takano[1], Shin-ya Miyauchi[1†], Yukinori Tsuchiya[1], Taro Saito[1], Ken-ichiro Kubo[2], Kazunori Nakajima[2], Mitsunori Fukuda[3], Mitsuharu Hattori[4] and Shin-ichi Hisanaga[1]*

[1]*Department of Biological Sciences, Tokyo Metropolitan University, Minami-osawa, Hachioji, Tokyo 192-0397, Japan*
[2]*Department of Anatomy, Keio University School of Medicine, Shinanomachi, Shinjuku-ku, Tokyo 160-8582, Japan*
[3]*Department of Developmental Biology and Neurosciences, Graduate School of Life Sciences, Tohoku University, Aobayama, Aoba-ku, Sendai, Miyagi 980-8578, Japan*
[4]*Department of Biomedical Science, Graduate School of Pharmaceutical Sciences, Nagoya City University, 3-1 Tanabe-dori, Mizuho-ku, Nagoya, Aichi 467-8603, Japan*

Reelin-Dab1 signaling is indispensable for proper positioning of neurons in mammalian brain. Reelin is a glycoprotein secreted from Cajal-Reztuis cells in marginal zone of cerebral cortex, and its receptors are Apolipoprotein E receptor 2 (ApoER2) or very low density lipoprotein receptor (VLDLR) expressed on migrating neurons. When Reelin binds to ApoER2 or VLDLR, an adaptor protein Dab1 bound to the receptors undergoes Tyr phosphorylation that is essential for Reelin signaling. We reported previously that Cdk5-p35 phosphorylates Dab1 at Ser400 and Ser491 and the phosphorylation regulates its binding to CIN85, which is an SH3-containing multiadaptor protein involved in endocytic downregulation of receptor-tyrosine kinases. However, the interaction of CIN85 with Dab1 has not been addressed in neurons. We examined here a possibility that CIN85 has a role in Reelin signaling. We found nonphosphorylated Dab1-mediated colocalization of CIN85 with ApoER2. The colocalization of CIN85 with ApoER2 was increased in neurons stimulated with Reelin repeats 3-6, an active Reelin fragment. The stimulation recruited CIN85 to domains in plasma membrane where it colocalized with ApoER2 and Dab1 and then to EEA1-labeled early endosomes in the cytoplasm. In addition, Tyr phosphorylation of Dab1 strengthened the binding to CIN85. These results suggest that CIN85 participates in Reelin signaling through the binding to Dab1.

Introduction

Proper neuronal positioning is a critical event during mammalian neocortical development. Newly born neurons migrate from their birth place at the ventricular and subventricular zones to their respective destination in the cortical plate (Jossin *et al.* 2004; Honda *et al.* 2011). During the migration, late generated neurons pass over previously located early born neurons. This sequential radial migration establishes the characteristic inside-out layering of cortical neurons. Studies on mutant mice with lamination defects have revealed a signaling cascade composed of Reelin, Apolipoprotein E receptor 2 (ApoER2) or very low density lipoprotein receptor (VLDLR), and Disabled-1 (Dab1), in neuronal migration and positioning (D'Arcangelo *et al.* 1999; Honda *et al.* 2011). Reelin is an extracellular glycoprotein secreted by Cajal-Retzius (CR) cells in the marginal zone, whereas ApoER2 and VLDLR are Reelin receptors expressed in migrating neurons and

Communicated by: Takeo Kishimoto
**Correspondence*: hisanaga-shinichi@tmu.ac.jp
[a]*Present address:* Center for Dementia Research, Nathan S. Kline Institute, 140 Old Orangeburg, NY 10962, USA.
[†]Deceased.

DOI: 10.1111/gtc.12045

Dab1 is a cytoplasmic adaptor protein that binds to ApoER2 or VLDLR (Stolt & Bock, 2006; Kubo *et al.* 2010). Binding of Reelin to ApoER2 or VLDLR induces tyrosine phosphorylation of Dab1 by Src family kinases (Hiesberger *et al.* 1999; Howell *et al.* 2000). Tyrosine phosphorylation of Dab1 transduces the signal to downstream cytoplasmic components including PI3K (Bock *et al.* 2003) and Crk family (Ballif *et al.* 2004). Although intensive studies have unraveled a number of possible signaling pathways, the regulation of Reelin receptor trafficking upon Reelin stimulation is largely unknown.

Cdk5, a member of cyclin-dependent kinase (Cdk) family, is a Ser/Thr kinase predominantly expressed in neurons. Cdk5 requires association with a neuron-specific activator p35 or p39 for kinase activity (Dhavan & Tsai 2001; Hisanaga & Endo 2010). Mice deficient in Cdk5 or p35 display inverted neuronal positioning in neocortical layers similar, but not identical, to mice with mutations in Reelin signaling pathway proteins (Ohshima *et al.* 2001). Although genetic approach has indicated that Cdk5-p35 and Reelin signaling pathways work in parallel (Ohshima *et al.* 2001; Beffert *et al.* 2004), there is also a direct interaction between them. Cdk5-p35 phosphorylates Dab1 at Ser400 and Ser491 (Keshvara *et al.* 2002; Sato *et al.* 2007), and this phosphorylation suppresses the tyrosine phosphorylation of Dab1 (Ohshima *et al.* 2007). We searched for proteins that interact with Dab1 in a Cdk5-dependent phosphorylation manner and identified Cbl-interacting protein of 85 kDa (CIN85, also known as Ruk, SETA, or SH3KBP1) and CD2-associated protein (CD2AP), both of which are SH3-containing adaptor proteins. The SH3 domains of CIN85 bind to the PxxxPR motif in the C-terminal region of Dab1 and that Dab1-CIN85 interaction was abolished by phosphorylation of Dab1 at Ser491 by Cdk5-p35 (Sato *et al.* 2007).

CIN85 and CD2AP constitute a family of adaptor molecules composed of N-terminal three SH3 domains and C-terminal proline-rich region and coiled-coil domain (Dikic 2002; Fig. S1 in Supporting Information). CIN85 plays a role in downregulation of activated receptor-tyrosine kinases (RTKs) such as epidermal growth factor receptor (EGFR), hepatocyte growth factor receptor and platelet-derived growth factor receptor via clathrin-dependent internalization (Petrelli *et al.* 2002; Soubeyran *et al.* 2002; Szymkiewicz *et al.* 2002). CIN85 is implicated to function as a scaffolding protein gathering endocytic proteins including E3 ubiquitin ligase Cbl, endophilin, and dynamin (Kowanetz *et al.* 2003a,b). CIN85 is also expressed abundantly in neurons but its neuronal function has not been analyzed sufficiently, whereas its role in dopamine receptor 2 internalization was shown recently by a study of CIN85-lacking mice (Shimokawa *et al.* 2010).

We investigated whether CIN85 interacts with Reelin receptors ApoER2 or VLDLR to participate in Reelin signaling in neurons. In fact, nonphosphorylated Dab1 mediated the association of CIN85 with ApoER2 or VLDLR in neurons. The results suggest that CIN85 has a role in the Reelin signalings through the intracellular trafficking of Reelin receptors in a Dab1-phosphorylation-dependent manner.

Results

CIN85 colocalizes with ApoER2 or VLDLR via nonphosphorylated Dab1

We examined whether CIN85 associates with the Reelin receptors ApoER2 and VLDLR by transient transfection in COS-7 cells. As was reported previously (Kirsch *et al.* 1999; Sato *et al.* 2007; Zhang *et al.* 2009), CIN85 formed large vesicle-like structures in the cytoplasm when over-expressed (Fig. 1A, arrows). In contrast, ApoER2-EGFP and VLDLR-EGFP accumulated at the perinuclear region (Fig. 1A, arrowhead) with diffuse and weak signals throughout the cytoplasm. When Dab1 was co-expressed with CIN85 and ApoER2-EGFP or VLDLR-EGFP, Dab1 wild type (WT) showed similar distribution to ApoER2 (Fig. 1B, b and c) or VLDLR (Fig. 1C, b and c), but not with CIN85 (Fig. 1B and C, a and c). However, when the non-phosphorylated Dab1 mutant Dab1-2A was co-expressed, ApoER2-EGFP or VLDLR-EGFP became localized on CIN85-positive large vesicles (Fig. 1B and C, e–h). These results indicate nonphosphorylated Dab1 at Ser400 and Ser491 mediates the interaction of ApoER2 or VLDLR with CIN85. We have performed most of the following experiments with both ApoER2 and VLDLR, but hereafter we will show only the results of ApoER2 with similar results for VLDLR presented in Supplemental figures to minimize the duplication and for clarity.

Expression and cellular distribution of endogenous CIN85 in cultured neurons

To investigate the cellular distribution of CIN85 in neurons, we expressed CIN85 exogenously in cultured cortical neurons. Upon over-expression, CIN85

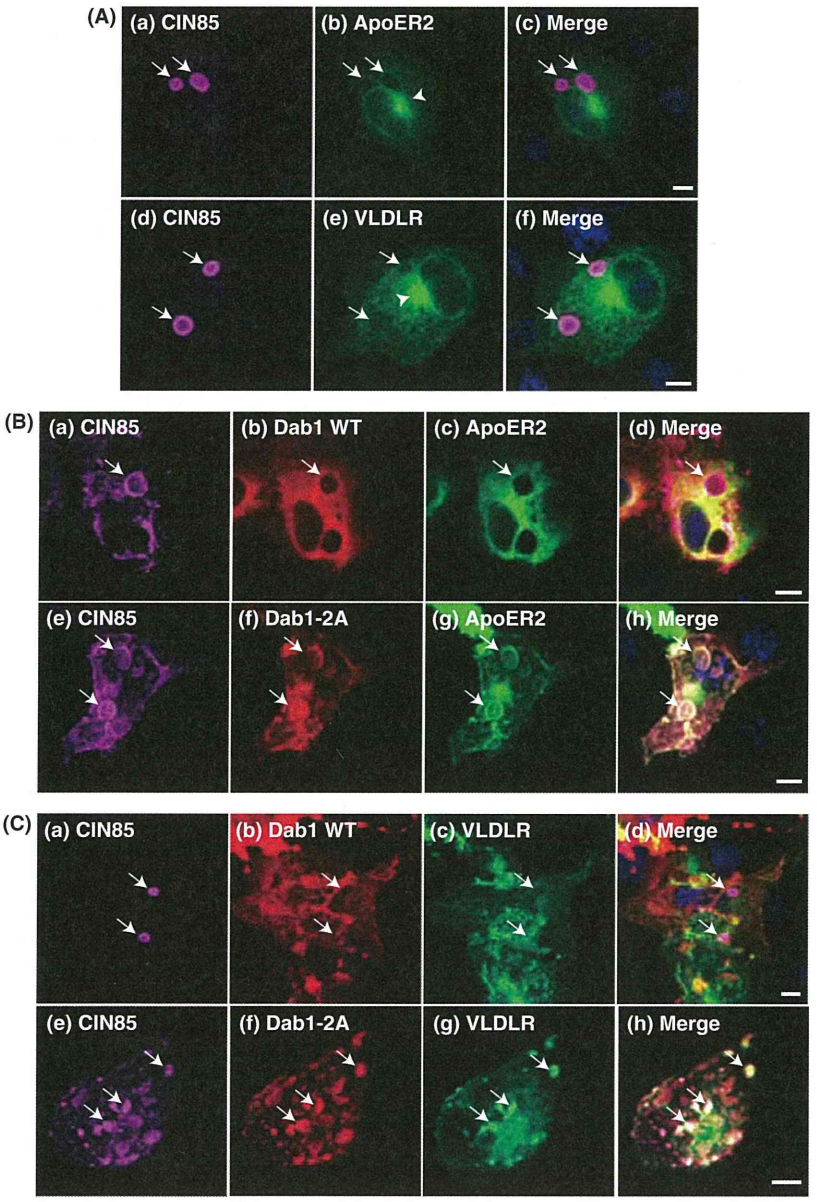

Figure 1 Dab1-2A mediates the association of CIN85 with Apolipoprotein E receptor 2 (ApoER2) or very low density lipoprotein receptor (VLDLR) in COS-7 cells. (A) Cellular localization of CIN85 and ApoER2 or VLDLR in COS-7 cells. COS-7 cells were transfected with HA-CIN85 and ApoER2-EGFP (a-c) or VLDLR-EGFP (d-f). CIN85 was immunostained with anti-HA followed by Alexafluor 647 conjugated secondary antibody and merged with EGFP of ApoER2 or VLDLR in (c) and (f). (B) and (C) Localization of ApoER2 to CIN85-induced large vesicles in the presence of Dab1-2A. COS-7 cells were transfected with ApoER2 (B) or VLDLR (C) with CIN85 in co-expressed with Myc-Dab1 wild type (WT) (a-d) or Myc-Dab1-2A (e-h). 24 h after transfection, cells were immunostained with anti-HA antibody for CIN85 and anti-Myc antibody for Dab1. Scale bars, 10 μm.

formed large vesicle-like structures in neurons (Fig. 2A) similar to those observed in COS-7 cells (Fig. 1). However, the formation of these large vesicular structures hampered our ability to analyze a role of CIN85 on Reelin-receptor trafficking. Thus, we decided to follow endogenous CIN85. To examine

the cellular distribution of endogenous neuronal CIN85, we generated anti-CIN85 antibody by immunizing rabbits with the C-terminal fragment of CIN85 (CIN85-CT, Fig. S1A). Affinity-purified anti-CIN85 recognized N-terminal FLAG-tagged CIN85-CT (Fig. 2B, lane 3 of a) but not CIN85 N-terminal fragment CIN85-NT (Fig. 2B, lane 2 of a). Full length of CIN85 was also detected by anti-CIN85 antibody (Fig. 2B, lane 2, double arrow of b), but FLAG-CD2AP, a family protein over-expressed in COS-7 cells, was not (Fig. 2B, lane 3 of b). A band indicated by an asterisk likely is derived from a degradation product, because the band was found only in a sample of CIN85 over-expression. The antibody also specifically detected endogenous CIN85 in COS-7 cells (Fig. 2B, a faint band indicated by arrow in lanes 1–3 of b) and mouse primary cortical neurons (Fig. 2B, arrow in lane 1 of c). Nonspecific bands were not observed with this antibody in a lysate of cultured neurons under this condition.

The specificity of the antibody was further confirmed by knocking CIN85 down in cultured neurons by shRNA. Knockdown vectors, CIN85-shRNA#1 and CIN85-shRNA#2, efficiently decreased expression levels of CIN85 in neurons when examined by immunoblotting with anti-CIN85 (Fig. 2C). Immunostainings are shown in Fig. 2D. The antibody stained small puncta distributed throughout the cell body and neurites. Large vesicles such as those seen in CIN85-transfected neurons (Fig. 2A) were not observed. The staining pattern is similar to that seen in cortical neurons stained with anti-CIN85 YH (Fig. S2 in Supporting Information, Kawata *et al.* 2006). Neurons transfected with

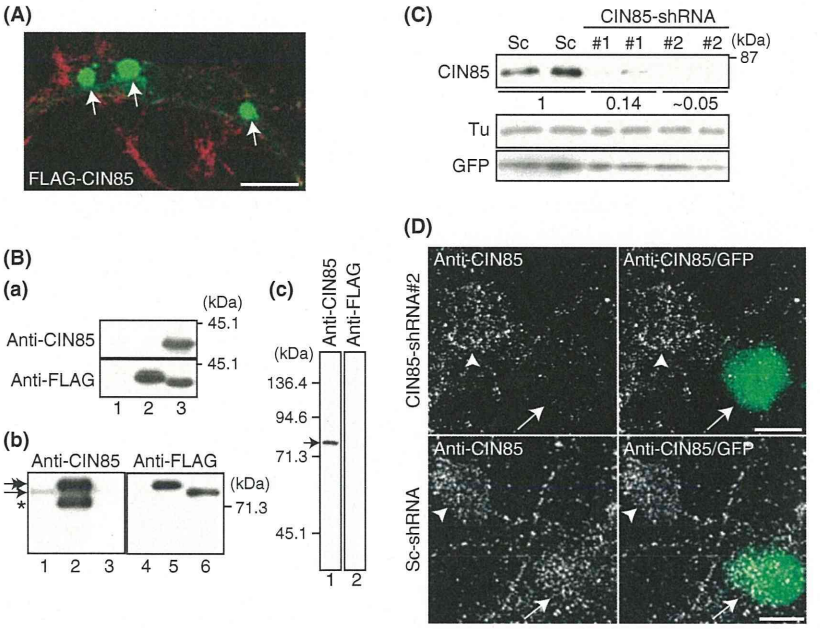

Figure 2 Large vesicle-like structures formed by CIN85 in cultured neurons and the specificity of anti-CIN85 antibody. (A) Large vesicle-like structures formed by over-expression of FLAG-CIN85 in neurons (arrows). CIN85 was immunostained with anti-FLAG antibody followed by Alexafluor 488-conjugated anti-rabbit IgG. F-actin was labeled with Rhodamine-Phalloidin. Scale bar, 10 μm. (B) Reactivity and specificity of anti-CIN85 antibody. (a) Immunoblotting of COS-7 cells transfected with empty vector (lane 1), FLAG-CIN85-NT (lane 2), or FLAG-CIN85-CT (lane 3). (b) Immunoblotting of COS-7 cells transfected with empty vector (lanes 1 and 4), FLAG-CIN85 (lanes 2 and 5), or FLAG-CD2AP (lanes 3 and 6) with anti-CIN85 (lanes 1–3) or anti-FLAG antibody (lanes 4–6). (c) Immunoblotting of a mouse cortical neuron lysate with anti-CIN85 antibody (lane 1) or anti-FLAG antibody (lane 2). (C) Knockdown of CIN85 in mouse cortical neurons by shRNA. Duplicates of each shRNA are shown. Sc is a control shRNA with a scramble sequence. GFP encoded in shRNA plasmid is a marker for transfection. Tubulin (Tu) is the loading control. Knockdown efficiency is indicated below a blot of CIN85. (D) Specificity of anti-CIN85 antibody in immunostaining of mouse cortical neurons. Neurons were transfected with CIN85-shRNA (upper panel) or Sc-shRNA (lower panel) together with GFP (arrow) encoded in the same vector. An untransfected neuron is indicated by arrowhead. Scale bars, 10 μm.

shRNA are identified by GFP expression (arrows in Fig. 2D). Anti-CIN85 signals were greatly reduced in a neuron transfected with CIN85-shRNA#2 (Fig. 2D, arrow, upper panels) but not scramble (Sc)-shRNA (Fig. 2D, arrow, lower panels).

Expression levels and localization of CIN85 in cultured cortical neurons

Using the anti-CIN85-specific antibody described above, we next examined expression levels and cellular distribution of endogenous CIN85 in cultured mouse cortical neurons. CIN85 was already detected in neuron cultures at 3 days *in vitro* (DIV). The expression levels of CIN85 gradually increased with culturing duration from three DIV to 12 DIV (Fig. 3A, upper panel). Dab1 was also expressed in the neuron cultures (Fig. 3A, middle panel). It is reported that CIN85 localizes in postsynaptic spines (Kawata *et al.* 2006; Shimokawa *et al.* 2010). To confirm it, we double-labeled primary cortical neurons with anti-CIN85 and anti-PSD-95 at 12 DIV, a time when synapses are formed in neuronal cultures. A fraction of CIN85 showed colocalization with PSD-95 (Fig. 3B, arrows), but many of the CIN85-positive puncta in cell body and dendrites were not stained with anti-PSD-95. There has been no previous description of this nonsynaptic localization of CIN85.

We examined in what membrane compartments CIN85 resides. Considering its role in endocytosis of EGFR in non-neuronal cells, we focused on various endosomes. Endosomal markers used here were Rab4A for early recycling endosomes, Rab5A for early endosomes, Rab7 for late endosomes, Rab8A for a subset of recycling endosomes, and Rab11A for recycling endosomes (Fukuda 2008). We also checked for localization of CIN85 to Golgi apparatus (Havrylov *et al.* 2008) using Golgi markers, GM130, and golgin97. There were some overlapping of CIN85 staining with all Rabs used here in the perinuclear region or on neurites, but most part of CIN85 showed limited colocalization with them (Fig. S3 in Supporting Information). CIN85 localized neither with GM130 nor golgin97 (Fig. S4 in Supporting Information). Thus, the primary membrane compartments where major part of CIN85 is present in are still unknown in neurons.

Dab1-mediated colocalization of CIN85 with ApoER2 in neurons

We examined the interaction of CIN85 with ApoER2 in cortical neurons by expressing ApoER2-EGFP exogenously. Fluorescence of ApoER2-EGFP

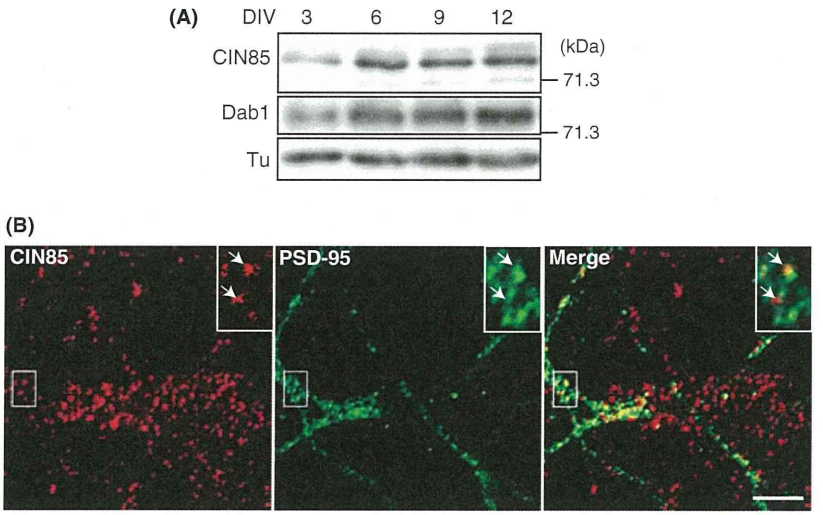

Figure 3 Expression and subcellular distribution of CIN85 in cultured cortical neurons. (A) Immunoblotting of the lysates of primary cortical neurons cultured for the indicated days with anti-CIN85 and anti-Dab1. Tubulin (Tu) is the loading control. (B) Immunostaining of cortical neurons at 12 days *in vitro* with anti-CIN85 and anti-PSD-95 antibodies, followed by Alexafluor 647-conjugated anti-rabbit IgG and Alexafluor 488-conjugated anti-mouse IgG, respectively. Merge is shown in the right. Inset shows a higher magnification view of the region indicated by rectangles. Scale bar, 5 μm.

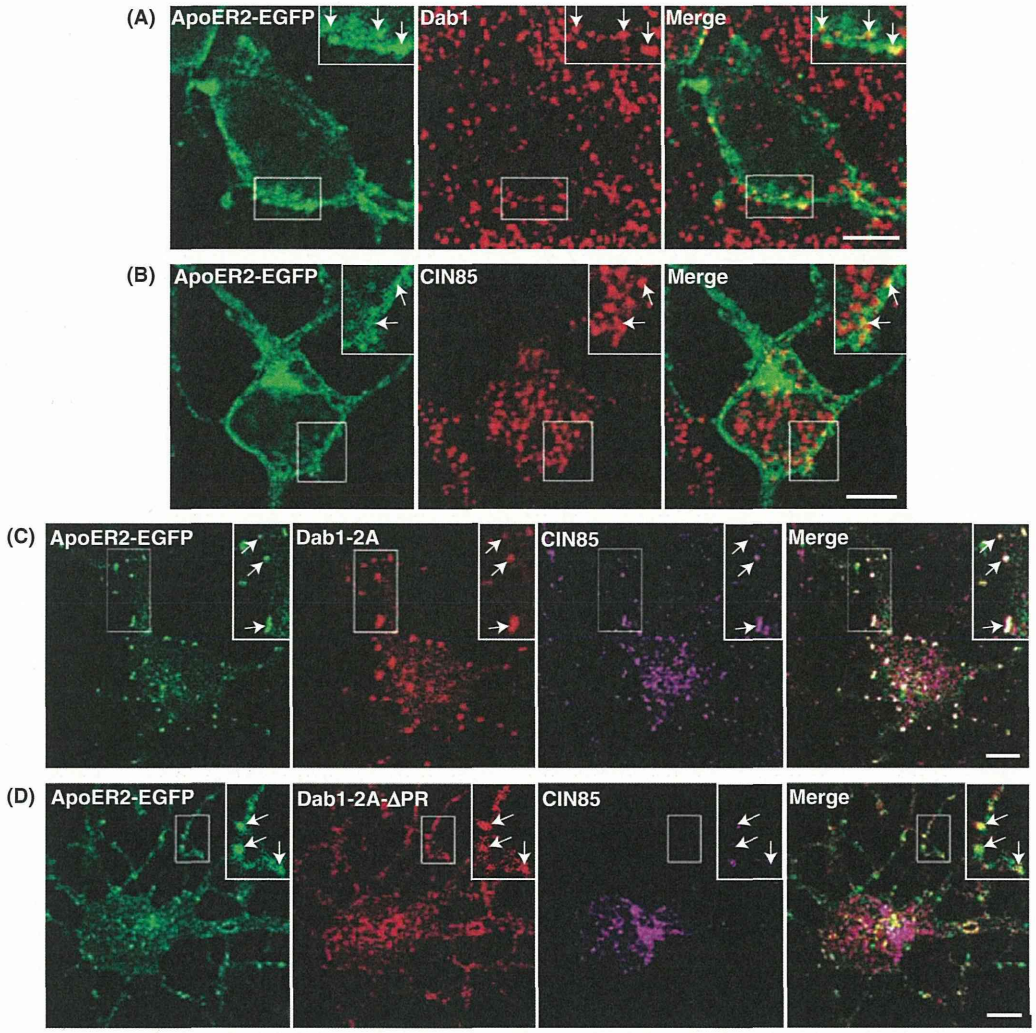

Figure 4 Association of CIN85 with ApoER2 in cultured neurons. (A) and (B) Distribution of ApoER2–EGFP and CIN85 or Dab1 in primary neurons. Cortical neurons expressing ApoER2-EGFP were immunostained with anti-Dab1 (A) or anti-CIN85 (B) antibody. Merge is shown in right panels. Inset shows a higher magnification of the region indicated by rectangles. Colocalization of ApoER2-EGFP with Dab1 or CIN85 is indicated by arrows. (C) and (D) Dab1-2A-mediated colocalization of ApoER2-EGFP and CIN85 in cortical neurons. Three days after transfection of ApoER2-EGFP and Dab1-2A (C) or Dab1-2A-ΔPR (D), distribution of ApoER2-EGFP, Dab1-2A, Dab1-2A-ΔPR, and CIN85 was examined. Inset shows a higher magnification of the region indicated by rectangles. Colocalization of ApoER2, Dab1 proteins, and CIN85 is indicated by arrows (C). Scale bars, 5 μm.

was found at both the cell surface and at the perinuclear region as reported (Beffert *et al.* 2005; Dumanis *et al.* 2012). Although Dab1 showed a degree of colocalization with ApoER2-EGFP around the cell periphery (Fig. 4A), CIN85 showed decreased level of colocalization with ApoER2-EGFP (Fig. 4B).

To examine whether Dab1-2A mediates the binding of CIN85 to ApoER2 in neurons as was observed in COS-7 cells, we expressed Dab1-2A with ApoER2-EGFP in primary neurons. Dab1-2A showed similar distribution to ApoER2-EGFP in neurons (Fig. 4C). In this case, CIN85 immunostainings was frequently observed with punctate ApoER2 and Dab1-2A localization both in the cytoplasm and in peripheral region of the cell body. ApoER2 was also found together with CIN85 and Dab1-2A in the neurites (Fig. 4C, arrows). As a negative control, we used Dab1-2A-ΔPR lacking the CIN85-binding

sequence ^{483}PTPAPR^{488}. The inability of Dab1-2A-ΔPR in binding to CIN85 is shown in COS-7 cells (Fig. S5 in Supporting Information). In neurons as well, Dab1-2A-ΔPR showed little colocalization with CIN85, whereas it showed a similar distribution to ApoER2 (Fig. 4D, arrows). Similar results were obtained with VLDLR (Fig. S6C and D in Supporting Information).

CIN85 colocalizes with Reelin repeats 3-6-ApoER2-Dab1 in neurons treated with Reelin repeats 3-6

We wanted to examine the association of CIN85 with ApoER2 when neurons were also exposed to Reelin. To observe all four components, CIN85, Dab1, ApoER2, and Reelin, together as a complex, we used a red fluorescent protein (RFP)-Reelin repeats 3-6 (RFP-RR3-6) construct that is a Reelin fragment composed of Reelin repeats 3-6 tagged with RFP (Yasui *et al.* 2007). RR3-6 is the active region of Reelin, which can bind and stimulate ApoER2 and VLDLR for signal transduction to downstream targets (Jossin *et al.* 2004; Yasui *et al.* 2007). Dab1-2A was also expressed to increase the interaction of CIN85 with ApoER2-EGFP, whereas Dab1-2A-ΔPR served as a negative control. When neurons expressing both ApoER2-EGFP and Dab1-2A were incubated with conditioned medium containing RFP-RR3-6 at 4 °C, RFP signals were observed at the periphery of neurons (Fig. 5A, arrows) and in the neurites (Fig. 5A, arrowheads),

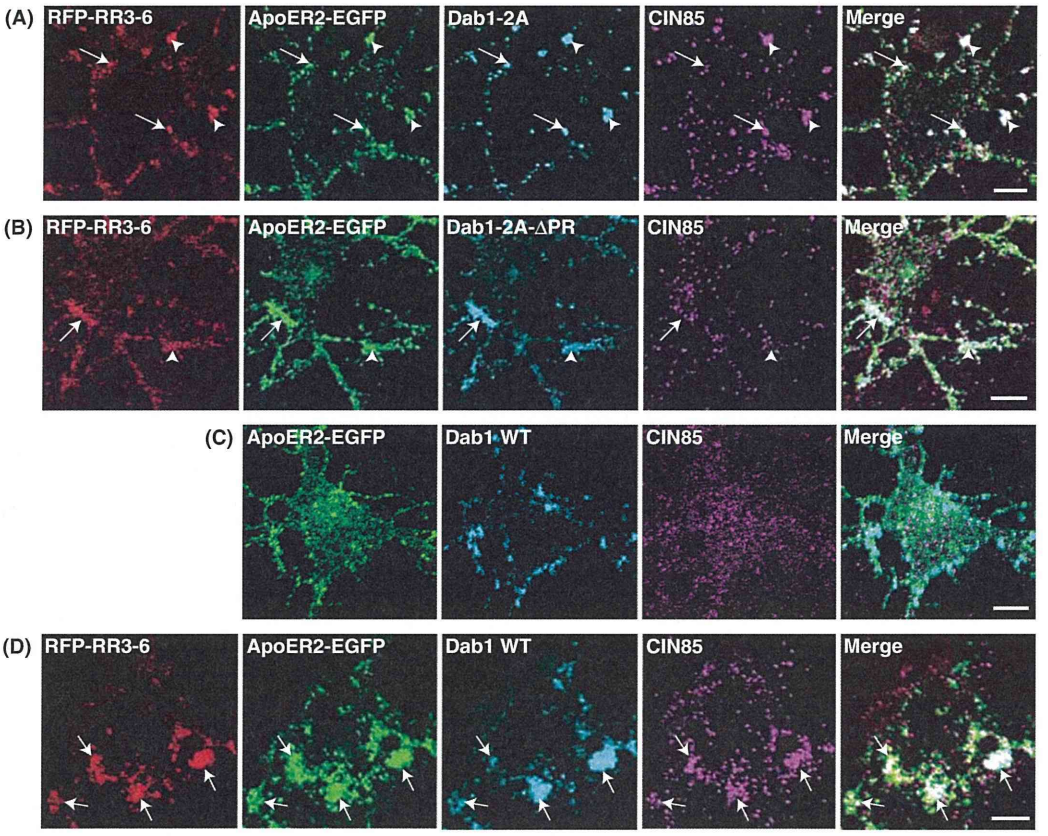

Figure 5 Localization of the RR3-6-ApoER2-Dab1-CIN85 complex in neurons. (A–B) Neurons expressing ApoER2-EGFP and Dab1-2A or Dab1-2A-ΔPR were placed at 4 °C for 15 min and then incubated with cold RFP-RR3-6-conditioned medium at 4 °C for 20 min. Dab1-2A or Dab1-2A-ΔPR were visualized by staining with anti-Myc antibody, and CIN85 was stained with anti-CIN85. (C–D) The effect of RFP-RR3-6 treatment on cellular localization of CIN85. Neurons expressing ApoER2-EGFP and Dab1 WT were immunostained with anti-Myc antibody for Dab1 and anti-CIN85 antibodies (C). After the treatment with RFP-RR3-6 as described in (A–B), neurons were immunostained with anti-Myc antibody for Dab1 and anti-CIN85 antibody (D). Colocalization of RFP-RR3-6, ApoER2-EGFP, Dab1 WT, and CIN85 was indicated by arrows. Scale bars, 5 μm.

where ApoER2 was found. CIN85 was colocalized at the same spots when Dab1-2A was co-expressed (Fig. 5A). In contrast, when Dab1-2A-ΔPR was used, the colocalization of CIN85 was decreased although a few colocalization was observed (Fig. 5B, arrow).

As Dab1-2A induced the binding of CIN85 to ApoER2 whether or not neurons were treated with RFP-RR3-6, we could not evaluate the effect of RFP-RR3-6 on the interaction between ApoER2 and CIN85. To avoid constitutive association, we introduced Myc-Dab1 WT into neurons exogenously. This made us possible to observe Dab1 and CIN85 at the same time, otherwise we could not because no antibodies for double staining of endogenous CIN85 and Dab1 are available. In these neurons, over-expressed Dab1 WT showed colocalization with ApoER2-EGFP, whereas CIN85 showed a few colocalization with ApoER2-EGFP or Dab1 WT (Fig. 5C). In contrast, after the treatment with RR3-6, CIN85 accumulated on ApoER2-EGFP and Dab1 WT where RFP-RR3-6 was also found (Fig. 5D, arrows). These results suggest that RFP-RR3-6 induces the formation of the signaling complex including ApoER2, Dab1, and CIN85 on surface of neurons.

Early endosome localization of internalized ApoER2-Dab1-CIN85 complex

We observed internalized RFP-RR3-6 in the cytoplasm of the cell body by treating neurons with RFP-RR3-6 at 37 °C for 5 min. RFP-RR3-6 was colocalized with ApoER2 and Dab1-2A in the region close to the nucleus, as well as CIN85 (Fig. 6A, upper panels, arrows). The XZ images along the line indicated in Merge are shown in lower panels. RFP-RR3-6 was found as a large cluster nearby the lower surface of neurons completely colocalized with ApoER2, Dab1-2A, and CIN85. In addition, signals of ApoER2 extended upward into the cytoplasm, where a faint signal of RR3-6 was also observed, whereas Dab1-2A and CIN85 were not (Fig. 6A, lower panels). CIN85 and Dab1 might be dissociated from internalized ApoER2 and RR3-6 complexes. In contrast, we observed little overlaps of CIN85 with RR3-6 and ApoER2 when Dab1-2A-ΔPR was co-expressed (Fig. 6B). Nevertheless, RR3-6 bound to ApoER2-EGFP was found in the cytoplasmic region close to the nucleus (Fig. 6B, in upper panels, arrows). The XZ-plane analysis again showed large vertical cluster of ApoER2, but CIN85 was not focused there (Fig. 6B). The results suggest that

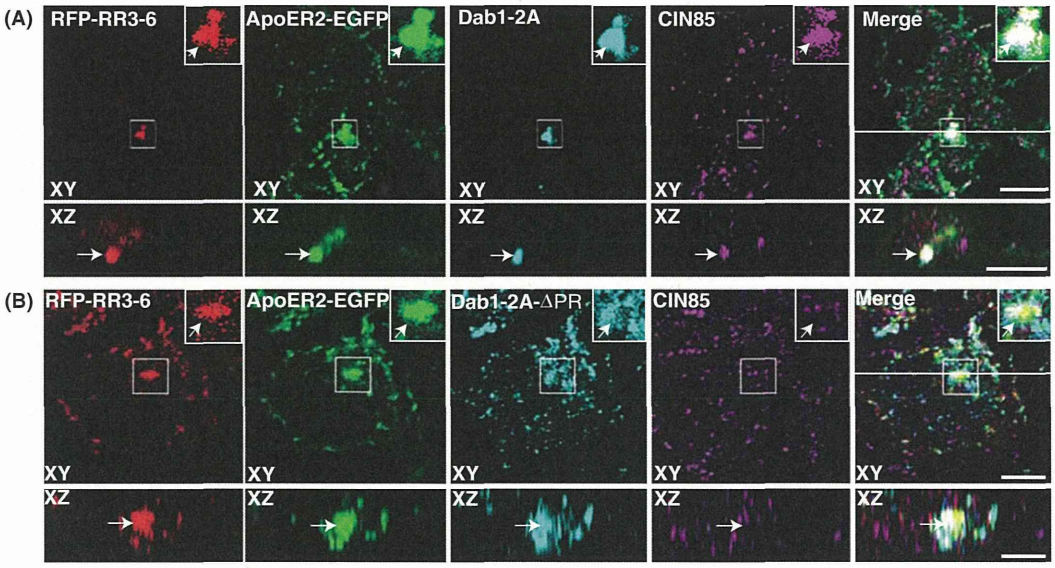

Figure 6 Internalization of RFP-RR3-6-ApoER2-Dab1 complex and CIN85 in cultured neurons. Neurons expressing ApoER2-EGFP and Dab1-2A (A) or Dab1-2A-ΔPR (B) were incubated with prewarmed RFP-RR3-6-conditioned medium at 37 °C for 5 min. CIN85 and Dab1 were observed as described above. Inset shows a higher magnification of the area indicated by rectangle. The XZ images along the line in Merges are shown in lower panels. Arrows indicate the colocalization of RFP-RR3-6, ApoER2-EGFP, Dab1-2A and CIN85 (A), and RFP-RR3-6, ApoER2-EGFP, and Dab1-2A-ΔPR in (B). Scale bars, 5 μm.

CIN85 really associates with Reelin-receptor complexes through Dab1.

CIN85 colocalized with the internalized RFP-RR3-6-ApoER2 complex in the cytoplasm (Fig. 6A). As noted earlier, however, we did not observe the clear localization of CIN85 on endosomes labeled by various Rabs in neurons in the absence of RR3-6 (Fig. S3 in Supporting Information). We next examined the localization of internalized Reelin-receptor complex in early endosomes using EEA1 as an early endosome marker. First, we confirmed that CIN85 was not present in EEA1-positive endosomes in the absence of RR3-6 (Fig. 7A). To make the complex of CIN85 with ApoER2 and Dab1, ApoER2 and Dab1-2A were over-expressed in Fig. 7B. Even though CIN85 bound to over-expressed ApoER2-EGFP and Dab1-2A, CIN85 was not colocalized with EEA1-positive early endosomes (Fig. 7B). However, upon RR3-6 treatment at 37 °C, CIN85 became detectable colocalized with RR3-6 and ApoER2 in EEA1-positive vesicles (Fig. 7C, arrows). These results suggest that Reelin-receptor signaling complexes containing CIN85 are internalized into early endosomes.

Tyrosine phosphorylation of Dab1 increases the interaction with CIN85

Phosphorylation of Dab1 at Ser400 or Ser491 by Cdk5 is not affected by Reelin stimulation (Keshvara *et al.* 2002; Sato *et al.* 2007). Nevertheless, RR3-6 showed the colocalization with CIN85 in neurons expressing ApoER2 and Dab1 WT (Fig. 5D). Reelin stimulation is manifested by Tyr phosphorylation of Dab1 (Howell *et al.* 2000). Thus, we next evaluated whether Tyr phosphorylation of Dab1 increases the interaction with CIN85. To visualize this interaction, we co-expressed Dab1-2A and CIN85 NT with Fyn in COS-7 cells. In this experiment, we used the N-terminal fragment of CIN85 consisting of three SH3 domains to minimize the formation of large-vesicle-like structures on the interaction. Phosphorylation of Dab1 at Tyr residues was confirmed by immunoblotting with anti-phospho-Tyr antibody (Fig. 8, 2nd panel, lane 2). When

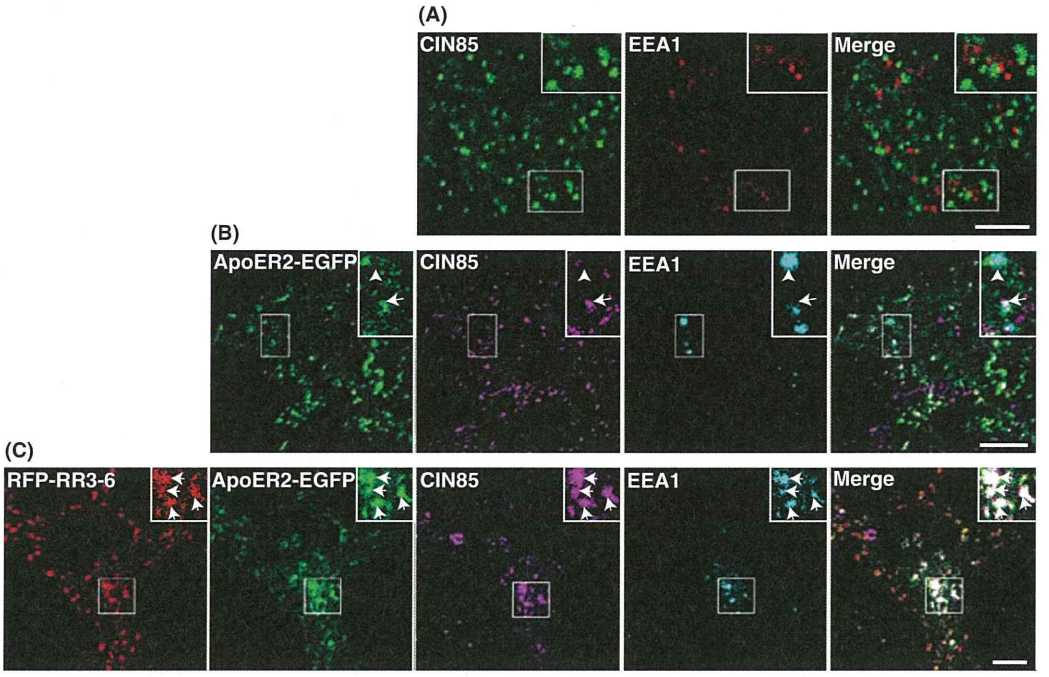

Figure 7 Localization of RFP-RR3-6-ApoER2-CIN85 in EEA1-positive early endosomes. (A) Cortical neurons were immunostained with anti-CIN85 and anti-EEA1 antibodies. Merge is shown in right panel. (B) Neurons expressing ApoER2-EGFP and Dab1-2A were immunostained with anti-CIN85 and anti-EEA1 antibodies at 3 days *in vitro*. EEA1 staining of putative endosomes lacking either ApoER2 or CIN85 is indicated by arrowhead. ApoER2-CIN85 colocalization without EEA1 staining is indicated by arrow. Merge is shown in right panel. (C) Neurons expressing ApoER2-EGFP and Dab1-2A were treated with RFP-RR3-6 at 37 °C for 15 min. CIN85 and EEA1 were probed as described in (B). Inset shows a higher magnification of the region indicated by rectangles. Scale bars, 5 μm.

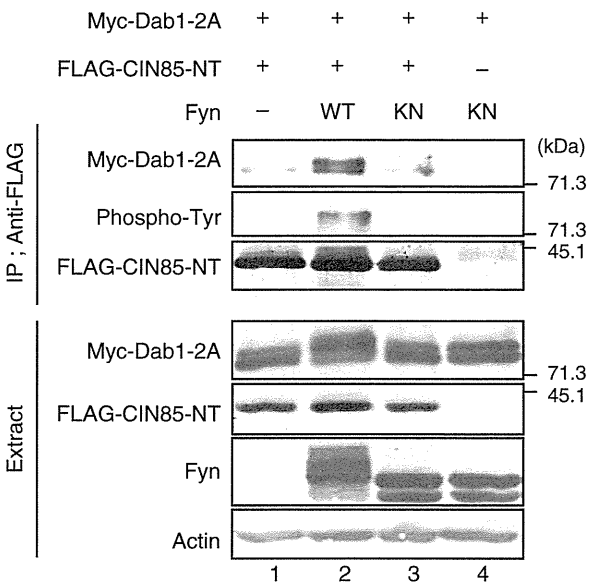

Figure 8 Tyr phosphorylation of Dab1 by Fyn increases its binding to CIN85-NT. COS-7 cells transfected with Myc-Dab1-2A, FLAG-CIN85-NT, and Fyn wild type or kinase negative were subjected to immunoprecipitation with anti-FLAG antibody. Immunoprecipitates were probed with anti-Myc for Dab1-2A, anti-phospho-Tyr (4G10) and anti-FLAG for CIN85.

CIN85-NT was immunoprecipitated, larger amount of Dab1-2A was found in the immunoprecipitates of CIN85-NT in the presence of Fyn WT compared with the kinase negative (KN) form of Fyn (Fig. 8, upper panel, lane3). The Tyr-phosphorylated Dab1-2A may correspond to the bands shifted upward in Myc-Dab1-2A in the extract (Fig. 8, 4th panel, lane 2). These results point to Tyr phosphorylation of Dab1 enhances the interaction of Dab1 with CIN85.

Discussion

We have previously reported the interaction of Dab1 with the CIN85 adaptor protein in a phosphorylation-dependent manner (Sato *et al.* 2007). However, this interaction has not been previously addressed in neurons. Using a specific antibody to CIN85, we studied the interaction and localization of CIN85 and Reelin-receptor complexes in cultured cortical neurons. Dab1-2A mediated the colocalization of CIN85 with ApoER2 and VLDLR. CIN85 was detected on punctate staining of Dab1 and ApoER2 or VLDLR along plasma membranes and on internalized vesicles in RR3-6-stimulated neurons. These results suggest that CIN85 is a novel component of the neuronal Reelin signaling complex.

CIN85 is an SH3-containing adaptor protein expressed broadly in many mammalian cells and tissues. It is well established that CIN85 plays an important role in endocytosis of RTK in a clathrin-dependent fashion for their down-regulation (Kowanetz *et al.* 2003a,b). CIN85 is also expressed abundantly in brains (Buchman *et al.* 2002; Shimokawa *et al.* 2010), but our understanding of its neuronal function is limited. We have shown here CIN85 colocalizes with ApoER2 or VLDLR via Dab1 in a phosphorylation-dependent manner in cultured cortical neurons. Reelin receptors ApoER2 and VLDLR are single transmembrane proteins with the NPxY motif in the cytoplasmic tail, to which a subset of adaptor proteins with PTB domains binds (Stolt & Bock, 2006; Marzolo & Bu 2009). Dab1 is such a PTB domain-bearing protein, mediating the Reelin signal into cytoplasmic effectors (Hiesberger *et al.* 1999). It has been shown that cell surface ApoER2 and VLDLR are internalized via clathrin-mediated endocytosis (Cuitino *et al.* 2005), and the NPxY sequence of ApoER2 and VLDLR is required for the clathrin-mediated endocytosis (Schneider & Nimpf 2003). However, the mechanism how ApoER2 or VLDLR is internalized remains to be clarified. Our data have suggested that CIN85 could be a factor regulating trafficking of Reelin receptors and Dab1 complex. In this respect, CIN85 may recruit endocytic proteins, such as Cbl and endophilin, to ApoER2 or VLDLR as is shown with receptor-type tyrosine kinases (Kowanetz *et al.* 2003a,b). Recently, CIN85 was shown to function in downregulation of dopamine receptor 2, a G-protein-coupled receptor, in striatal neurons (Shimokawa *et al.* 2010). Taken together, these results suggest that CIN85 may act as an adaptor protein involved in the internalization of various types of membrane receptors.

In addition, CIN85 may also be involved in recruitment of the ApoER2 or VLDLR and Dab1 complexes from internal membrane compartments to cell surface. In unstimulated neurons, CIN85 showed a punctate distribution throughout the cytoplasm. However, the identity of the vesicles has not been verified. CIN85 is reported to be present in Golgi apparatus in adherent cultured human cells (Havrylov *et al.* 2008), but in neurons Golgi is not a major site that CIN85 resides. CIN85 is reported to localize to Rab7-positive late endosome (Schroeder *et al.* 2010), and CD2AP, another family member of SH3-containing proteins along with CIN85, is shown to interact with the active form of Rab4 (Cormont *et al.*

2003). However, CIN85 only showed an overlap distribution marginally with any of endosomal markers at the perinuclear region and neurites when wild-type Rab proteins expressed. Thus, the identity of the vesicles, with which most of CIN85 associates in neurons, is not indicated yet. The colocalization of CIN85 with ApoER2 or VLDLR was markedly enhanced when co-expressed with Dab1-2A (Fig. 4C, Fig. S6C in Supporting Information). After the treatment with RR3-6, a part of CIN85 colocalized with ApoER2 and Dab1 on plasma membrane (Fig. 5D). It is reported that ApoER2 at the cell surface increases in the presence of Dab1 without change in total expression levels (Morimura *et al.* 2005; Hoe *et al.* 2006), and Dab1 affects trafficking of ApoER2 to cell surface in COS-7 cells expressing Dab1 and ApoER2 (Hoe *et al.* 2006). These results suggest that Dab1 promotes plasma membrane localization of Reelin receptors. The present results further explore the notion that CIN85 cooperates with Dab1 to promote plasma membrane localization, at least in part, of ApoER2 and VLDLR.

Tyrosine phosphorylation of Dab1 induced by Reelin stimulation is an essential step for transducing the signal to cytoplasmic downstream effectors. Importantly, we show that the RR3-6 treatment increased the colocalization of CIN85 with ApoER2 or VLDLR and co-expression of Fyn strengthened the interaction between CIN85 and Dab1 likely by inducing Tyr phosphorylation of Dab1. This is reminiscent of CIN85 binding to Cbl that is enhanced by growth factor-induced tyrosine phosphorylation of Cbl (Take *et al.* 2000; Soubeyran *et al.* 2002; Kowanetz *et al.* 2003a,b). Tyrosine phosphorylation sites are present in the middle of Cbl and the PxxxPR sequence is in its C-terminal site. Tyrosine phosphorylation is considered to induce a conformational change of Cbl protein, leading to opening or stabilization of the PxxxPR motif. The similar mechanism may also occur in the interaction between Dab1 and CIN85. However, Tyr phosphorylation sites themselves are the binding sites on Dab1 for several downstream proteins such as PI3K and Crk. Crk is a multi-adaptor protein containing SH2 and SH3 domain that associate with a particular set of phospho-Tyr residues in Dab1 (Huang *et al.* 2004; Matsuki *et al.* 2008; Park & Curran 2008). PI3K p85, a well-known cell survival factor upstream of Akt, also binds to another set of phospho-Tyr residues of Dab1 (Bock *et al.* 2003). Proteomic interaction assays suggest that CIN85 also associates directly with PI3K p85 and Crk (Watanabe *et al.* 2000). These results point to a scenario wherein Reelin-induced Tyr phosphorylation of Dab1 promotes the association of CIN85 with ApoER2 through assembly of signaling elements including Crk and PI3K. Most recently, it was shown that the interaction of CIN85 with Dab1 is regulated by phosphorylation of CIN85 (Bior & Ballif 2013). Taken together, these data implicate CIN85 as a novel component in a scaffold assembling in the Reelin-Dab1 signaling pathway which is regulated by multiple protein phosphorylation.

CIN85 binds to Dab1 at ^{483}PTPAPR^{488} sequence in the C-terminal region, and this binding is inhibited by phosphorylation of Dab1 at nearby Ser491 via Cdk5-p35 (Sato *et al.* 2007). Cdk5 also mediates the cellular signaling in control of cortical lamination (Ohshima *et al.* 2001); raising the postulate that there exists crosstalk between Reelin and Cdk5 signalings has been a question to be investigated. Compound mutants on genes in Reelin and Cdk5 signalings showed the increased abnormality of layer formation in several brain areas, compared to those with a single deficiency (Ohshima *et al.* 2001; Beffert *et al.* 2004), suggesting their genetic interaction. In contrast, levels of Reelin and Dab1 were not altered in Cdk5−/− mouse brains (Ohshima *et al.* 2001), and vice versa, levels of Cdk5 activity were unchanged in Reeler (Keshvara *et al.* 2002; Sato *et al.* 2007). Phosphorylation of Dab1 by Cdk5 was the first biochemical evidence to implicate the crosstalk (Keshvara *et al.* 2002; Ohshima *et al.* 2007), followed by isolation of CIN85, which binds to Dab1 in a Cdk5-dependent phosphorylation manner (Sato *et al.* 2007). The present results further extend their interaction to those including ApoER2 and VLDLR, and suggest a role for CIN85 in trafficking of ApoER2 or VLDLR. Related to cellular function of Cdk5, we would like to note that Cdk5 regulates the trafficking of recycling endosomes in axons by phosphorylation of LMTK1/AATYK1, a novel Ser/Thr kinase residing on recycling endosomes (Takano *et al.* 2012). Thus, Cdk5 may play a role in endosomal dynamics in neurons by phosphorylating proteins on respective endosomes.

To see a role for CIN85 in endocytosis of Reelin receptors, we have knocked CIN85 down using shRNA and assessed its effect on internalization of RFP-RR3-6 in primary neurons. Although the internalized RFP-RR3-6 was reduced slightly in neurons transfected with CIN85-KD shRNA compared with Sc-shRNA, there was no significance between them (Fig. S7 in Supporting Information). Considering a report describing that only a small percentage of ApoER2 is affected in trafficking by Dab1 (Hoe *et al.*

2006), CIN85 may be involved in recruitment of only a subset of Reelin receptors in embryonic neurons. Alternatively, CD2AP would have compensated the decrease of CIN85 in knockdown neurons. This is implicated by the fact that CD2AP, as well as CIN85, in the rat brain extract binds to Dab1-2A (Sato *et al.* 2007). Otherwise, the role of CIN85 in endocytosis of ApoER2 or VLDLR might be demonstrated more clearly in an experiment using adult neurons. In this respect, the Reelin-ApoER2 signaling is suggested to function in synaptic activity in adult brains (Weeber *et al.* 2002; Beffert *et al.* 2005). There is no developmental deficiency as shown in mice lacking CIN85, but those mice do show deficiency in dopamine receptor 2 endocytosis in adults (Shimokawa *et al.* 2010). Depending on the amount and species of adaptor proteins assembling to Reelin receptors, the internalization may be differentially regulated (Duit *et al.* 2010). In addition, we note recent studies that CIN85, as well as CD2AP, is implicated as risk factors in Alzheimer disease (Hollingworth *et al.* 2011; Naj *et al.* 2011; Treusch *et al.* 2011). It is shown that ApoER2 regulates the trafficking and the proteolytic processing of amyloid precursor protein (APP) that correlates deeply with Aβ production (Fuentealba *et al.* 2007; He *et al.* 2007; Durakoglugil *et al.* 2009). It is a fascinating hypothesis that CIN85 and CD2AP may affect APP processing by regulating ApoER2 or VLDLR trafficking.

Experimental procedures

Antibodies

Anti-FLAG M2, anti-actin, and Rhodamine-Phalloidin were purchased from Sigma-Aldrich (St. Louis, MO). Anti-HA Y11, anti-Myc 9E10, and anti-Fyn antibodies were obtained from Santa Cruz Biotechnology (Santa Cruz, CA, USA). Anti-Myc polyclonal antibody was purchased from Cell Signaling (Danvers, MA, USA). Anti-EEA1 and anti-GM130 antibodies were from B.D. Biosciences (Franklin Lakes, NJ). Anti-golgin97 was purchased from Molecular Probe (Eugene, OR, USA). Anti-PSD-95 antibody was purchased from Thermo Scientific (Waltham, MA, USA). Anti-GFP monoclonal antibody was from Roche (Penzberg, German). Anti-Tubulin (Tuj-1) antibody was purchased from TECHNE Corporation (Cambridge, UK). Anti-phospho-Tyrosine (4G10) was from Millipore (Billerica, MA, USA). Horse radish peroxidase (HRP)-conjugated or alkaline phosphatase (AP)-conjugated anti-mouse IgG and anti-rabbit IgG were purchased from Covance (Princeton, NJ, USA). Alexa Fluor 405, 488, 546, or 647-conjugated anti-mouse or anti-rabbit IgG were obtained from Invitrogen (Carlsbad, CA, USA). The polyclonal anti-CIN85 antibody was raised against the C-terminal 327-665 amino acids fragment of CIN85 and affinity-purified using the CIN85 C-terminal fragment conjugated to NHS-activated HP column (GE Healthcare, Buckinghamshire, UK). Anti-CIN85 YH antibody was provided from Dr. Y. Hata at Tokyo Medical and Dental University (Tokyo, Japan). Anti-Dab1 antibody was described previously (Sato *et al.* 2007), and anti-Reelin repeat 5A antibody was described previously (Yasui *et al.* 2007).

Expression or knockdown vectors

Expression vectors encoding mouse ApoER2 or VLDLR tagged with EGFP at their C-terminus was provided from Dr. J. Nimpf at University of Vienna (Vienna, Austria). CIN85, CIN85-NT, or CIN85-CT was inserted in pFLAG-CMV2 or pcDNA3-3xHA. pSecTag-RFP-Reelin repeats 3-6 and pcDNA3-Myc-Dab1 are described previously (Sato *et al.* 2007; Yasui *et al.* 2007). CIN85 knockdown targeting vectors were constructed by the insertion of shRNA sequences into pcDNA6.2-GW/EmGFP (Invitrogen). Targeted sequences were 5′-GGTTTGTTCCCTGACAACTTT-3′ for shRNA#1 and 5′-AATGGGAAGACTGGAATGTTT-3′ for shRNA#2, corresponding to nucleotide sequence 136-156 and 421-441 of mouse CIN85 cDNA, respectively. A vector encoding scramble sequence provided from Invitrogen was used as a negative control. shRNA targeting vectors without GFP were constructed by removing the nucleotide sequence of GFP from the shRNA vector at *Dra*I restriction sites.

Cultures of mouse cortical neurons and cell lines, and transfection

COS-7 cells and HEK293T cells were maintained in Dulbecco's Modified Eagle Medium supplemented with 10% fetal bovine serum. Transfection was performed using Lipofectamine2000 (Invitrogen), Polyfect (Qiagen, Hilden, Germany), or HilyMax (Dojindo, Kumamoto, Japan) according to the methods of manufacturer's instruction. Primary cortical neurons were prepared from brains of ICR mice (Sankyo lab, Tokyo, Japan) at embryonic days 14–16. All experiments were performed according to the guidelines for animal experimentation of Tokyo Metropolitan University. Neurons were cultured in Neurobasal medium (Invitrogen) containing 2% B-27 supplement (Invitrogen) and 0.5 mM Glutamine, 50 U/ml Penicillin G and 0.1 mg/mL Streptomycin as described previously (Endo *et al.* 2009). Transient transfection into primary neurons was performed with an AMAXA Nucleofector II (Roche) before seeding (Takano *et al.* 2012).

Preparation of Reelin repeats 3-6-containing conditioned medium and treatment of neurons

Conditioned medium containing RFP-RR3-6 was prepared by transient transfection into HEK293T cells and cultured for

3 days. Medium was collected and sterilized with 0.22 μm filter as described previously (Yasui *et al.* 2007). Expression of RFP-RR3-6 was confirmed by immunoblotting with anti-Reelin repeat 5A. Neurons were treated with the conditioned medium containing RR3-6 by replacing half of culture medium with the conditioned medium for indicated duration at 4 or 37 °C.

Immunofluorescence staining, immunoprecipitation, and immunoblotting

Primary neurons and COS-7 cells on coverslips were fixed with 4% paraformaldehyde in phosphate-buffered saline (PBS) at room temperature for 25 min. After washing with PBS, cells were permeabilized with 0.1% Triton X-100 in PBS for 5 min and treated with 1% nonfat skimmilk in PBS for 10 min to block nonspecific immunoreactions. Then cells were incubated with the indicated primary antibodies at 4 °C for overnight. After washing with PBS, cells were further incubated with Alexafluor-conjugated secondary antibodies at 37 °C for 1 h. Specimens were analyzed with a confocal microscopy, LSM510 Exciter or LSM710 (Carl Zeiss, Oberkochen, Germany).

COS-7 cells expressing FLAG-CIN85 NT, Myc-Dab1-2A, and Fyn or kinase negative Fyn (Fyn KN) were lysed in Hepes buffer (20 mM Hepes, pH 7.4, 100 mM NaCl, 5 mM MgCl2, 1 mM EGTA, 10% glycerol, 1% Triton X-100, 10 μg/mL Leupeptin, 1 μM E64, 400 μM 4-(2-Aminoethyl) benzenesulfonyl fluoride, 1 mM DTT, 1 mM Na_3VO_4). FLAG-CIN85 NT was immunoreacted with anti-FLAG M2 antibody and collected with Protein G Sepharose 4B (GE Healthcare) Fast Flow as previously described (Sato *et al.* 2007). Immunoblotting was performed as described previously (Sato *et al.* 2007). After blocking with 5% of nonfat milk in TBS-T, membranes were reacted with anti-Myc or anti-FLAG antibody followed by HRP-conjugated secondary antibodies. Immunoreactivity was detected with Immobilon chemiluminescent HRP Substrate (Millipore, Billerica, MA, USA).

Acknowledgements

We would like to express our thanks to J. Nimpf at University of Vienna for providing ApoER2-EGFP and VLDLR-EGFP and Y. Hata at Tokyo Medical and Dental University for providing anti-CIN85 YH antibody. We thank Martin J. Berg at Nathan S. Kline Institute for reading the manuscript. This work was supported in part by Grants-in-Aid for Scientific Research from MEXT, Japan (S.H.).

References

Ballif, B.A., Arnaud, L., Arthur, W.T., Guris, D., Imamoto, A. & Cooper, J.A. (2004) Activation of a Dab1/CrkL/C3G/Rap1 pathway in Reelin-stimulated neurons. *Curr. Biol.* **14**, 606–610.

Beffert, U., Weeber, E.J., Durudas, A., Qiu, S., Masiulis, I., Sweatt, J.D., Li, W.P., Adelmann, G., Frotscher, M., Hammer, R.E. & Herz, J. (2005) Modulation of synaptic plasticity and memory by Reelin involves differential splicing of the lipoprotein receptor ApoER2. *Neuron* **47**, 567–579.

Beffert, U., Weeber, E.J., Morfini, G., Ko, J., Brady, S.T., Tsai, L.H., Sweatt, J.D. & Herz, J. (2004) Reelin and cyclin-dependent kinase 5-dependent signals cooperate in regulating neuronal migration and synaptic transmission. *J. Neurosci.* **24**, 1897–1906.

Bior, B.K. & Ballif, B.A. (2013) Dab1 stabilizes its interaction with Cin85 by suppressing Cin85 phosphorylation at serine 587. *FEBS Lett.* **587**, 60–66.

Bock, H.H., Jossin, Y., Liu, P., Foster, E., May, P., Goffinet, A.M. & Herz, J. (2003) Phosphatidylinositol 3-kinase interacts with the adaptor protein Dab1 in response to Reelin signaling and is required for normal cortical lamination. *J. Biol. Chem.* **278**, 38772–38779.

Buchman, V.L., Luke, C., Borthwick, E.B., Gout, I. & Ninkina, N. (2002) Organization of the mouse Ruk locus and expression of isoforms in mouse tissues. *Gene* **295**, 13–17.

Cormont, M., Meton, I., Mari, M., Monzo, P., Keslair, F., Gaskin, C., McGraw, T.E. & Marchand-Brustel, Y.L. (2003) CD2AP/CMS regulates endosome morphology and traffic to the degradative pathway through its interaction with Rab4 and c-Cbl. *Traffic* **4**, 97–112.

Cuitino, L., Matute, R., Retamal, C., Bu, G., Inestrosa, N.C. & Marzolo, M.P. (2005) ApoER2 is endocytosed by a clathrin-mediated process involving the adaptor protein Dab2 independent of its raft's association. *Traffic* **6**, 820–838.

D'Arcangelo, G., Homayouni, R., Keshvara, L., Rice, D.S., Sheldon, M. & Curran, T. (1999) Reelin is a ligand for lipoprotein receptors. *Neuron* **24**, 471–479.

Dhavan, R. & Tsai, L.H. (2001) A decade of CDK5. *Nat. Rev. Mol. Cell Biol.* **2**, 749–759.

Dikic, I. (2002) CIN85/CMS family of adaptor molecules. *FEBS Lett.* **529**, 110–115.

Duit, S., Mayer, H., Blake, S.M., Schneider, W.J. & Nimpf, J. (2010) Differential functions of AppoER2 and very low density lipoprotein receptor in Reelin signaling depend on differential sorting of the receptors. *J. Biol. Chem.* **285**, 4896–4908.

Dumanis, S.B., Chamberlain, K.A., Jin Sohn, Y., Jin Lee, Y., Guénette, S.Y., Suzuki, T., Mathews, P.M., Pak, D.Ts., Rebeck, G.W., Suh, Y.H., Park, H.S. & Hoe, H.S. (2012) FE65 as a link between VLDLR and APP to regulate their trafficking and processing. *Mol. Neurodegener.* **7**, 9.

Durakoglugil, M.S., Chen, Y., White, C.L., Kavalali, E.T. & Herz, J. (2009) Reelin signaling antagonizes beta-amyloid at the synapse. *Proc. Natl Acad. Sci. USA* **106**, 15938–15943.

Endo, R., Saito, T., Asada, A., Kawahara, H., Ohshima, T. & Hisanaga, S. (2009) Commitment of 1-methyl-4-phenylpyrinidium ion-induced neuronal cell death by proteasome-mediated degradation of p35 cyclin-dependent kinase 5 activator. *J. Biol. Chem.* **284**, 26029–26039.

Fuentealba, R.A., Barria, M.I., Lee, J., Cam, J., Araya, C., Escudero, C.A., Inestrosa, N.C., Bronfman, F.C., Bu, G. &